

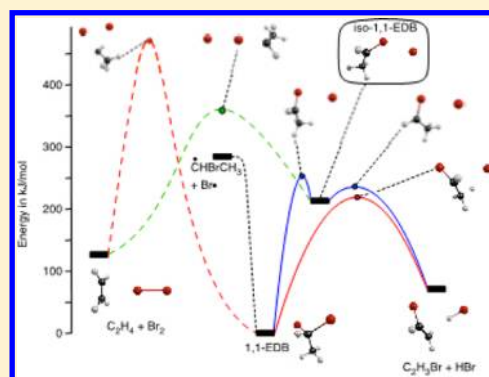
Case of the Missing Isomer: Pathways for Molecular Elimination in the Photoinduced Decomposition of 1,1-Dibromoethane

Aimable Kalume, Lisa George, Nicole Cunningham, and Scott A. Reid*

Department of Chemistry, Marquette University, Milwaukee, Wisconsin 53201-1881, United States

S Supporting Information

ABSTRACT: We report an experimental and computational study of the photodecomposition pathways of a prototypical gem-dihalide, 1,1-dibromoethane (1,1-EDB), in the condensed phase. Following photolysis of the matrix isolated parent compound in Ar at 5 K, photoproducts are observed corresponding to Br₂ elimination (+ C₂H₄ or C₂H₂) and HBr elimination (+ vinyl bromide). The elimination products are observed in the matrix as complexes. In contrast to our recent studies of the photolysis of matrix isolated polyhalomethanes, no evidence for the iso-1,1-EDB species is found, although studies of the matrix isolated 1,1-dibromo-2,2,2-trifluoroethane analogue show that the isomer is the dominant photoproduct. These results are examined in the light of theoretical studies that have characterized in detail the 1,1-EDB potential energy surface (PES). For Br₂ elimination, a pathway from the isomer on the singlet PES is found which involves a simultaneous Br₂ loss with 1,2-hydrogen shift; this pathway lies lower in energy than a concerted three-center elimination from the parent 1,1-EDB. For HBr elimination, our previous theoretical studies [Kalume, A.; George, L.; Cunningham, N.; Reid, S. A. *Chem. Phys. Lett.* **2013**, *556*, 35–38] have demonstrated the existence of concerted (single-step) and sequential pathways that involve coupled proton and electron transfer, with the sequential pathway involving the isomer as an intermediate. Here, more extensive computational results argue against a simple radical abstraction pathway for this process, and we compare experimental and computational results to prior results from the photolysis of the structural isomer, 1,2-EDB. These steady-state experiments set the stage for ultrafast studies of the dynamics of this system, which will be important in unraveling the complex photodecomposition pathways operative in condensed phases.



INTRODUCTION

The chemistry and photochemistry of polyhaloalkanes (halons) continues to receive much attention, due to their role in the chemistry of the atmosphere and environment, where significant biogenic, geogenic, and anthropogenic sources of C₁–C₃ halogenated compounds are known.^{1–4} The chemistry of even simple halons is remarkably diverse, owing in part to the unique properties of the halogens. For example, in condensed phases simple halomethanes are known upon irradiation to form isomers (the iso-halons) that feature a halogen–halogen bond^{5–25} and are best represented as ion-pairs between a halide anion and halocarocation.^{23,25} These are unique systems where isomerization is intimately linked to electron transfer.²³ Such isomerization can occur in condensed phases from simple geminate recombination upon cleavage of a C–X bond, yet our recent studies have shown that a well-defined reaction path links the two isomers,²³ and photoisomerization is a facile event.²⁴ Tarnovsky and co-workers have recently shown in ultrafast studies of the solution phase photolysis of CHBr₃ that a direct, concerted *excited state* isomerization pathway exists, arising from a conical intersection between the S₁ state of CHBr₃ and the S₀ state of iso-CHBr₃.²⁶ These iso-halons can be strongly bound, of the order of 40–60 kJ/mol,²³ and have been shown to be important reactive

intermediates in the photochemistry of halons in condensed phases. For example, iso-CH₂Br₂ (not the CH₂Br radical) is the methylene transfer agent in the photoinitiated cyclopropanation reaction of CH₂Br₂ and C₂H₄.¹¹

Can such isomers exist for larger (i.e., >C₁) halons? Here, the presence of multiple, competing rearrangement channels may limit their importance. However, the participation of iso-dihaloethanes in the early time dynamics following ultrafast excitation of 1,2-C₂H₄I₂ and 1,2-C₂F₄I₂ has been suggested.²⁷ Moreover, Ihee and co-workers have identified iso-1,2-C₂H₄I₂ as a solution phase intermediate in time-resolved X-ray diffraction studies of the photolysis of 1,2-C₂H₄I₂, and their calculations indicate that the isomer might be best described as an ethylene–I₂ van der Waals complex derived from I atom addition to a bridged iodoethyl radical.^{28–30} This is reminiscent of our studies of CF₂I₂, where iso-CF₂I₂ corresponds to a shallow minimum on the CF₂I₂ potential energy surface (PES) that is nearly isoenergetic with (and separated by a small barrier from) a van der Waals complex between CF₂ and I₂.²⁰

Special Issue: Curt Wittig Festschrift

Received: March 29, 2013

Revised: July 12, 2013

Published: July 12, 2013

Like their iodo-analogues, the 1,1- and 1,2-dibromoethanes are prototypical systems for understanding the photochemistry of larger halons. The photolysis of 1,2-dibromoethane (1,2-EDB) has been studied quite extensively in the gas-phase,^{31–33} with continuing controversy concerning the decomposition pathways. Molecular beam experiments using photofragment translational spectroscopy with excitation at $\lambda = 234$,^{34,35} 248,³³ and 267 nm^{34,35} show a three body asynchronous dissociation producing ethylene and two Br atoms. However, in bulk gas samples at low pressure, Chang and co-workers have identified a Br₂ elimination pathway with a quantum yield of 0.36 ± 0.18 , which was suggested to arise on the ground state potential energy surface (PES) through a 4-center transition state (TS).³² We recently studied the photolysis of 1,2-EDB in Ar and Ne matrixes at low temperature³⁶ and found that irradiation with 220 nm laser light led to Br₂ and C₂H₄ as the primary photoproducts.³⁷ We found no evidence for iso-1,2-EDB and suggested that reaction occurred via the classical C₂H₄Br radical,³⁶ which, however, was not trapped.

In comparison with 1,2-EDB, less is known about its structural isomer, the gem-dihalide 1,1-dibromoethane (denoted as 1,1-EDB).^{33,38} Molecular beam experiments show that 248 nm excitation induces a simple C–Br bond rupture.³³ In bulk gas samples at low pressure, Chang and co-workers again have identified a Br₂ elimination pathway with a quantum yield of 0.05 ± 0.03 , much smaller than that of 1,2-EDB.³² This was suggested to arise on the ground state potential energy surface (PES) through a 3-center transition state, with the calculated TS energy lying slightly above the photon energy. Motivated by our failure to trap iso-1,1-EDB in rare gas matrixes and the observation instead of HBr as a significant photoproduct in steady-state experiments, we recently reported a theoretical study of halogen halide (HBr) elimination pathways on the ground state PES of 1,1-EDB.³⁹ This study clearly demonstrated the existence of two distinct mechanisms for HBr production, each involving coupled electron and proton transfer. A concerted proton-coupled electron transfer (PCET) pathway was found to be favored by ~ 30 kJ/mol over a sequential electron transfer/proton transfer mechanism involving the iso-1,1-EDB as an intermediate. Importantly, these studies predict that the isomer is a minimum on the 1,1-EDB potential energy surface (PES), but the barrier to HBr elimination lies below that of isomerization.

In this work, we report the full experimental and theoretical results of our study of the photodecomposition pathways of 1,1-EDB in rare gas matrixes at low temperature. We find that the photochemistry is dominated by elimination to molecular products. Such pathways cannot be fully explained by simple radical–radical reactions of the initial photolytically generated species, but instead plausibly involve iso-1,1-EDB as a key intermediate, which is supported by experiments where the elimination pathways are blocked by substitution. Similarly, high level theory predicts the iso-species to be actively involved in the molecular decomposition of 1,1-EDB in condensed phases.

■ EXPERIMENTAL AND COMPUTATIONAL METHODS

The experimental methodologies used in this work have been described in detail in earlier publications.^{21,36} Briefly, a mixture of 1,1-EDB in Ar or Ne ($\sim 1:500$) was deposited onto the cold KBr window held at ~ 5 K using the pulsed deposition method with a solenoid activated pulsed valve (Parker-Hannifan,

General Valve Division, Iota-1). Typical deposition conditions were 1 ms pulse duration, 5 Hz repetition rate, 1–2 h deposition time, and 1 bar backing pressure.

Following deposition, the cold window was irradiated with laser light at 220 nm, generated from the frequency doubled output of a dye laser system (Lambda-Physik Scanmate 2E) operating on Coumarin 440 dye, pumped by the third harmonic (355 nm) of a Nd:YAG laser (Continuum NY-61). In other experiments, light at 240 nm was used, generated from the same laser system operated on Coumarin 480 dye. In either case, the photolysis beam was expanded using a 4:1 beam expander to fill the cold window and avoid damage to the KBr windows of the cryostat. Typical irradiation times were 0.5–1 h. Infrared spectra were obtained with an FTIR spectrometer (Nicolet 6700 model) equipped with a DTGS detector, which was purged at a flow rate of 20 L/min using a purge gas generator (Parker-Balston 75-52A). IR spectra were recorded at 1 cm^{−1} resolution and typically averaged over 128 scans. UV–visible spectra (200–1100 nm) were obtained using an Agilent diode array spectrophotometer, with a typical integration time of 1 s. All spectra were referenced to the cold sample window, and subsequently transferred to a spreadsheet and analysis program (Origin 8.0) for workup.

Under the assumption that the IR and UV/visible spectra sample the same region of the matrix, the integrated IR and UV/vis intensities were combined with calculated IR intensities to estimate the oscillator strength of the UV/vis transitions. Thus, the integrated IR absorbance of a given feature was divided by the calculated intensity (in km/mol) to derive a column density in the matrix, and an average value was obtained over the observed IR absorptions. The oscillator strength of a given electronic (UV/visible) band was then obtained according to the following formula.⁴⁰

$$f = \frac{\int A_{UV}(v) dv}{N_{IR}} \times (1.87 \times 10^{-7} \text{ mol/km}) \quad (1)$$

where N_{IR} is the column density derived from the IR measurements, and the numerator represents the integrated ultraviolet absorbance (over cm^{−1}).

Calculations were carried out on a local (Pere) 128 node cluster using the Gaussian 09 suite of electronic structure programs.⁴¹ Geometry optimizations of various stationary points on the 1,1-EDB PES were performed using density functional theory (typically the M062x functional) and MP2 methods in combination with a correlation consistent aug-cc-pVTZ basis set. Our past experience has shown that the optimized geometries of iso-halons obtained from DFT and MP2 wave functions can exhibit significant differences; however, the DFT methods are known to provide reliable vibrational frequencies. In all cases, the wave functions were tested for stability, and those found to be unstable were subjected to additional calculations carried out with spin-unrestricted methods. The extent of spin-contamination of the UHF wave functions was in each case negligible, as reflected in $\langle S^2 \rangle$ values of 0. Subsequently, single-point energy calculations were performed at the CCSD(T) level of theory on the optimized structures, with zero-point energy (ZPE) corrections calculated at the DFT level. To model the effects of solvation, calculations were also carried out in solvent (Ar) using the polarizable continuum model (PCM). Our prior calculations reported stationary points in vacuum and in dichloromethane using the PCM;³⁹ in practice, the difference in energies

between the vacuum and PCM(Ar) calculations was less than 10 kJ/mol, and significant only for stationary points involving significant charge separation. Binding energies of complexes were corrected for the effects of basis set superposition error (BSSE)⁴² using the counterpoise method; the BSSE corrections were typically of the order of 1 kJ/mol. Electronic absorptions and oscillator strengths were calculated using time-dependent DFT methods, with the M062x and CAM-B3LYP density functionals, which were previously benchmarked for similar species.^{23,25}

Using data from these calculations, we modeled the relative reaction rates using microcanonical transition state (RRKM) theory as implemented in the ChemRate program.⁴³ In the RRKM treatment,⁴⁴ the microcanonical rate constant at a given energy is represented by the expression

$$k(E, J) = \frac{1}{h} \frac{N^\ddagger(E - E_0)}{\rho(E, J)} \quad (2)$$

The numerator in eq 1 reflects the number of open channels at the transition state at a given energy above the critical reaction threshold (E_0), and the denominator is the density of reactant states at that energy.

RESULTS AND DISCUSSION

Figure 1 displays the difference infrared spectrum obtained after photolysis of a freshly deposited matrix (1:500 1,1-EDB/Ar)

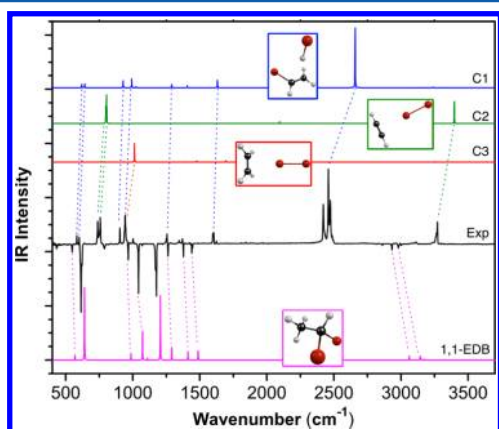


Figure 1. Calculated (M062x/aug-cc-pVTZ, unscaled) infrared spectra of 1,1-EDB and selected photoproducts together with experimental difference spectrum (black, exp) following photolysis of matrix isolated 1,1-EDB in Ne at 5 K. Upon photolysis, bands due to 1,1-EDB decrease in intensity, while bands due to various elimination products appear. These products are observed in the matrix as complexes, and include $\text{HBr} \cdots \text{CH}_2\text{CHBr}$ (C1), $\text{C}_2\text{H}_2 \cdots \text{Br}_2$ (C2), and $\text{C}_2\text{H}_4 \cdots \text{Br}_2$ (C3).

with 220 nm laser light (black, exp). Upon photolysis, peaks due to 1,1-EDB decreased in intensity, and new peaks were observed arising from molecular elimination products, which are observed in the matrix as complexes. The fact that these peaks increased in intensity upon annealing the matrix to 32 K and recooling back down to 5 K suggested that they belong to stabilized species. Also shown in Figure 1 are calculated spectra of the precursor (1,1-EDB) and representative photoproduct complexes (C1–C3) at the M062x/aug-cc-pVTZ level of theory. Considering the $\text{HBr} + \text{vinyl bromide}$ channel, our gas-phase calculations find five distinct minima for this complex, four of which exhibit intense HBr stretches due to the participation of the hydrogen atom in the noncovalent

interaction. The optimized structures of these complexes are shown in Figure S1 (Supporting Information), while Table S1 gives the calculated vibrational frequencies and infrared intensities for all five complexes, and Table S2 gives the calculated binding energies (corrected for ZPE and BSSE) using MP2 and CCSD(T) methods. In Figure 1, a representative IR spectrum of one of these complexes is shown (C1), which demonstrates a good correlation with our experimental results (Table 1).

Also apparent in the spectrum shown in Figure 1 are absorptions, at 739, 758, and 3271 cm^{-1} , that are in good agreement with the calculated spectrum (C2) of the $\text{Br}_2 \cdots \text{acetylene}$ complex (Table 1). In addition, a feature at 943 cm^{-1} that is overlapped with absorptions of the $\text{HBr} \cdots \text{vinyl bromide}$ complex signifies the presence of $\text{Br}_2 \cdots \text{ethylene}$ complex (C3), which we have recently studied in detail.³⁷ Thus, the IR spectra show the formation of products arising from distinct elimination pathways to HBr and Br_2 .

Further evidence for the formation of Br_2 is provided by spectra in the UV–visible region, shown in Figure 2. The parent 1,1-EDB has a band in the UV region at $\sim 218 \text{ nm}$ ($f = 0.015$); the observed position and intensity of this band are in excellent agreement with theory (Table 2). After 0.5 h of photolysis using light at a wavelength of 220 nm (trace labeled PP in Figure 2), this band decreased in intensity, and a new band appeared at $\sim 392 \text{ nm}$, which is assigned to molecular Br_2 .⁴⁵ After annealing the matrix to 32 K and recooling to 5 K, a feature at $\sim 233 \text{ nm}$ (trace labeled PA in Figure 2) grows in at the expense of the 392 nm feature, corresponding to the $\text{Br}_2 \cdots \text{C}_2\text{H}_4$ complex that we have reported in our previous work.³⁶ From solution phase (CH_3CN) spectra of dilute Br_2 solutions, we estimate the oscillator strength of the Br_2 visible ($X^1\Sigma_g^+ - B^3\Pi_u$) absorption to be ~ 0.007 , or roughly 1/2 that of the 1,1-EDB band. The ratio of integrated absorptions in the postphotolysis (PP) spectrum in Figure 2 is in rough accord with this expectation. Note that the corresponding charge transfer band of the acetylene complex and bands of the $\text{HBr} \cdots \text{vinyl bromide}$ complex were not observed since the strongest absorptions are predicted to appear deeper in the UV region (Table 2) and our experimental setup did not allow for measurement below 200 nm.

These steady-state experiments provide clear evidence for two different elimination pathways in the steady-state photolysis of 1,1-EDB in condensed phases; but what of the isomer? No evidence was found for the trapping of iso-1,1-EDB in these experiments. Calculations (Table S3, Supporting Information) of the IR spectra predict that the strongest band of the isomer is near 718 cm^{-1} , but no feature at this position is apparent. Similarly, TDDFT calculations (Table 2) predict the strongest band to occur near 350 nm ($f = 0.45$, Table 2). No feature at this position is observed in the postphotolysis spectrum (trace PP, Figure 2), although a very weak absorption (i.e., reflecting some trace amount of isomer formation) could lie hidden under the Br_2 band. Given that the isomer is a minimum on the 1,1-EDB PES, our failure to trap it in detectable yield suggests that either it is not formed or that it reacts on a time scale fast compared with the rate of vibrational relaxation in the matrix. To check the former, we conducted studies of the selectively fluorinated analogue, 1,1-dibromo-2,2,2-trifluoroethane (1,1-DB-2,2,2-TFE). In this case, the isomer is the only observed photoproduct following 240 nm excitation (Figure 3), providing indirect evidence that our failure to trap the isomer of 1,1-EDB is due to its fast reaction,

Table 1. Calculated and Observed Vibrational Frequencies (in cm^{-1}) and Intensities (Calculated Intensity in Parentheses, Unit = km/mol) of Species Relevant to This Work

species	M062x/aug-cc-pVTZ	MP2/aug-cc-pVTZ	observed	relative intensity
HBr...CH ₂ CHBr (complex 1)	31 (0.2)	30 (0.2)		
	67 (0.5)	76 (0.6)		
	77 (1)	88 (0.3)		
	355(5)	260 (3)		
	361 (0.4)	307 (3)		
	450 (4)	351 (0.1)		
	622 (18)	619 (17)	583	4
	636 (23)	642 (18)	601	4
	971 (42)	928 (34)	904	8
	1000 (37)	992 (43)	943	6
	1030 (8)	1025 (7)	1002	4
	1290 (21)	1291 (17)	1254	8
	1415 (9)	1408 (10)	1371	2
	1685 (47)	1631 (42)	1600	16
	2687 (212)	2659 (318)	2422, 2459, 2472	100
	3157 (1)	3182 (0.7)		
	3223 (0.6)	3242 (4)		
	3252 (0.6)	3289 (0.3)		
Br ₂ ...C ₂ H ₄	59 (0)	70 (0.2)		
	60 (0.2)	71 (0.4)		
	111 (10)	107 (19)		
	129 (0.2)	140 (0.3)		
	190 (0.3)	222 (0.5)		
	323 (13)	304 (24)		
	835 (0)	823 (0)		
	1013 (158)	936 (0)	943	100
	1021 (0)	983 (152)		
	1069 (0)	1049 (0)		
	1244 (0)	1242 (0)		
	1384 (4)	1370 (7)	1345	6
	1477 (11)	1475 (9)		
Br ₂ ...C ₂ H ₂	1695 (16)	1653 (18)	1623	5
	3150 (3)	3174 (2)		
	3164 (1)	33189 (0.5)		
	3229 (0)	3266 (0)		
	3255 (40)	3292 (2)		
	52 (0.1)	56 (0.1)		
	55 (0.1)	58 (0.2)		
	111 (4)	100 (7)		
	131 (0.5)	108 (0.6)		
	328 (7)	324 (9)		
	716 (0)	597 (0)		
	723 (0.1)	597 (0)		
	800(84)	752 (78)	739	69
	805 (141)	759 (132)	758	100
	2095 (10)	1955 (7)		
	3398 (111)	3422 (111)	3271	70
	3512 (0.2)	3521 (0.1)		

in competition with vibrational cooling and back-isomerization. Ultrafast studies of related systems show that after photolysis the vibrationally hot isomer is formed within 1–2 ps and cools into its potential well on the 10–50 ps time scale.^{24,46,47}

Our previous theoretical report indicated a very low barrier to HBr loss from the isomer, and to estimate the time scale for this reaction, we used microcanonical RRKM theory; the full

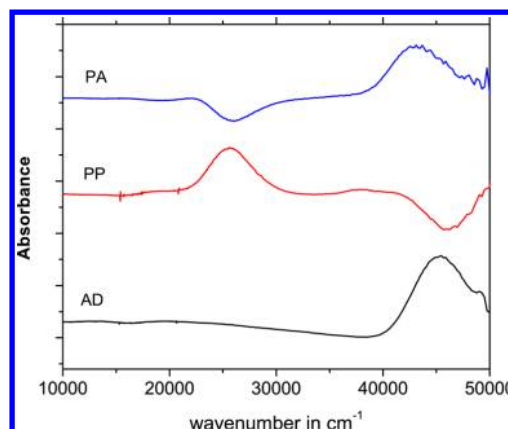


Figure 2. UV–visible spectra of matrix isolated 1,1-dibromoethane as deposited at 5 K (black, AD), a difference spectrum recorded postphotolysis at 220 nm (red, PP), and a spectrum recorded postannealing to 32 K and recooling to 5 K (blue, PA).

Table 2. Observed and Calculated Electronic Absorptions (in nm) and Oscillator Strength (f , in Parentheses) of Species Relevant to This Work

species	TD-M062x	TD-CAM-B3LYP	observed
HBr...CH ₂ CHBr (complex 1)	207.3 (0.0005)	206.4 (0.0014)	
	195.2 (0.1527)	194.9 (0.1933)	
C ₂ H ₄ –Br ₂	406.4 (0.0005)	406.2 (0.0006)	
	404.4 (0.0003)	404.8 (0.0004)	
	230.3 (0.0005)	235.7 (0.0004)	
	224.5 (0.5335)	231.3 (0.5291)	233
C ₂ H ₂ –Br ₂	412.5 (0.0005)	413.0 (0.0006)	
	407.2 (0.0004)	408.7 (0.0005)	
	232.7 (0.0003)	237.6 (0.0005)	
	230.3 (0.0003)	235.5 (0.0002)	
	210.6 (0.0018)	217.8 (0.0016)	
	206.0 (0.5175)	213.3 (0.4420)	
1,1-EDB	221.8 (0.0176)	221.0 (0.0180)	218(0.015)
	216.0 (0.0000)	213.8 (0.0000)	
	209.0 (0.0007)	207.6 (0.0007)	
iso-1,1-EDB	493.9 (0.0002)	493.7 (0.0003)	
	458.2 (0.0013)	459.0 (0.0022)	
	345.5 (0.4454)	350.0 (0.4492)	
	271.3 (0.0020)	269.6 (0.0018)	
1-bromoethyl radical	234.5 (0.0007)	231.0 (0.0006)	
	214.7 (0.0511)	212.5 (0.0521)	
	314.8 (0.0018)	297.3 (0.0018)	
	257.6 (0.0004)	259.8 (0.0000)	
	255.0 (0.0000)	248.7 (0.0010)	
	230.0 (0.0067)	227.9 (0.0477)	
1-bromo-2,2,2-trifluoroethyl radical	224.4 (0.0442)	220.0 (0.0092)	
	220.1 (0.0049)	211.1 (0.0056)	
	288.9 (0.0000)	296.2 (0.0000)	
	274.4 (0.0005)	262.5 (0.0004)	
	246.8 (0.0567)	248.3 (0.0595)	
	208.1 (0.0001)	203.4 (0.0001)	
	194.1 (0.0001)	198.1 (0.0001)	
	192.3 (0.0003)	191.8 (0.0004)	

results of these calculations are provided in Figure S2 in the Supporting Information. While it is certainly possible that the energy distribution in the nascent isomer is not ergodic,⁴⁸ the calculated vibronic density of states of the isomer at the excess

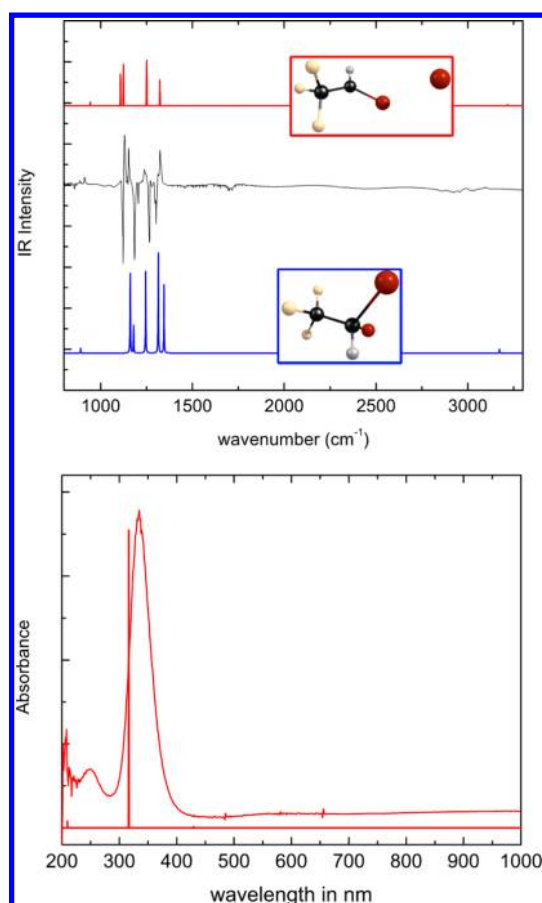


Figure 3. IR (top) and UV–visible spectra obtained following photolysis of 1,1-dibromo-2,2,2-trifluoroethane isolated in an Ar matrix at 5 K. Shown as stick spectra are calculated spectra of the parent and iso-form at the (TD) M06-2x/aug-cc-pVTZ level. These spectra show that iso-1,1-dibromo-2,2,2-trifluoroethane is the sole photoproduct.

energy of our experiment is of the order of $10^6/\text{cm}^{-1}$. Studies of a related system, CH_2I_2 , in solution have shown IVR lifetimes of ~ 10 ps for state densities of the order of $10^2/\text{cm}^{-1}$.⁴⁸ From our RRKM calculations, the predicted rate for HBr loss from the isomer is on the ps time scale, showing that HBr elimination from the hot-isomer may effectively compete with vibrational cooling.

What, then, are the mechanisms for molecular elimination in 1,1-EDB, and how is the iso-1,1-EDB species involved? Beginning first with the Br_2 channel, a concerted mechanism where two C–Br bonds break and Br–Br bond forms simultaneously is the least plausible because of the high energy three-center transition state (~ 420 kJ/mol at the CCSD(T)//MP2/aug-cc-pVTZ//PCM(Argon) level) leading to singlet methylcarbene, as shown in the stationary point diagram in Figure 4. Rather, we assume that photon absorption leads initially to homolytic cleavage of the C–Br bond and formation of a $\text{CH}_3\text{CHBr}^\bullet/\text{Br}^\bullet$ radical pair trapped within the matrix cage, although a direct photochemical pathway to iso-1,1-EDB similar to that recently found in CHBr_3 cannot be excluded.²⁶ One then envisions a radical mediated abstraction producing Br_2 in concert with (singlet) methylcarbene, which rearranges to ethylene by a 1,2-hydrogen shift. At the energy of our experiment, the nascent ethylene is unstable with respect to H_2 loss and some fraction will decompose to give acetylene,

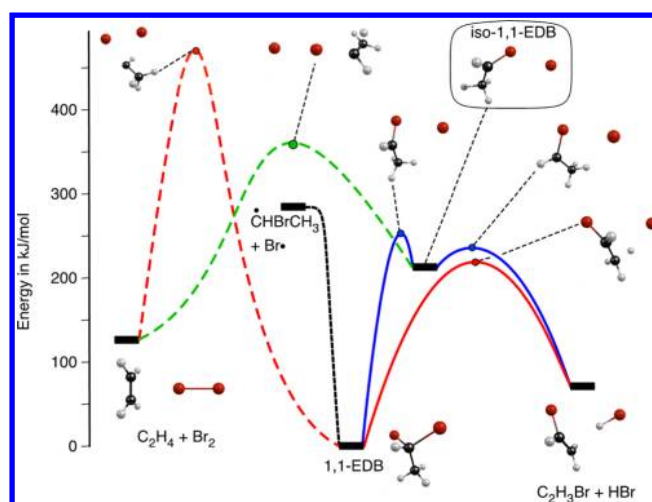


Figure 4. Stationary points on the 1,1-EDB potential energy surface, calculated at the CCSD(T)//MP2/aug-cc-pVTZ//PCM(argon) level. Pathways to Br_2 (left) are shown as dashed lines.

accounting for the range of products observed. It is known that singlet CH_3CH , which is a minimum on the PES that lies some 10 kJ/mol above the ground triplet state,⁴⁹ can easily isomerize to ethylene with a barrier of about ~ 8 kJ/mol⁵⁰ or decompose into $\text{C}_2\text{H}_2 + \text{H}_2$ with a relative barrier of ~ 140 kJ/mol.⁵¹

While a radical mediated process is reasonable, any attack of the liberated Br atom on the bound Br atom in the radical must access the region of the PES corresponding to iso-1,1-EDB and thus should (at least transiently) access the isomer well. The possible role of the isomer (and electron transfer) cannot therefore be neglected, irrespective of whether a direct photochemical pathway exists.²⁶ Earlier studies of the dibromomethanes have shown that Br_2 loss from the isomer is a barrierless process,^{21,22} and thus, we envision a concerted pathway involving simultaneous Br_2 loss with a 1,2-hydrogen shift from the isomer. Is such a pathway plausible? Theory suggests that it is. A transition state connecting the isomer well to the Br_2 (+ ethylene) product was found, and intrinsic reaction coordinate (IRC) calculations at the M062x/aug-cc-pVTZ level confirm the reaction path (Figure 5). The calculated vibrational frequencies of this TS are given in Table S4, Supporting Information. Stationary points on the 1,1-EDB PES, calculated at the CCSD(T)//M062x/aug-cc-pVTZ//PCM(argon) level (Figure 4), show that the Br_2 elimination pathway from iso-1,1-EDB (green dashed line) lies far lower in energy than a concerted 3-center pathway from the parent 1,1-EDB (red dashed line). In the gas-phase study of Chang and co-workers,³² isomer formation was not considered as a possible mechanism for Br_2 production; however, we recently showed that isomerization can explain the yield of molecular products observed in the infrared multiple photon dissociation (IRMPD) of CF_2Cl_2 and CF_2Br_2 .²² The existence of a direct excited state photochemical pathway to that isomer, such as recently demonstrated in CHBr_3 , may provide another explanation.²⁶

The discussion thus far has not considered the possible effects of secondary photolysis. Two potential intermediates might absorb at the 220 nm photolysis wavelength: iso-1,1-EDB and 1-bromoethyl radical. Indeed, TDDFT calculations (Table 2) predict that the strongest absorption of the radical in the UV region occurs near 220 nm, while iso-1,1-EDB has a predicted absorption of moderate strength at 215 nm. We

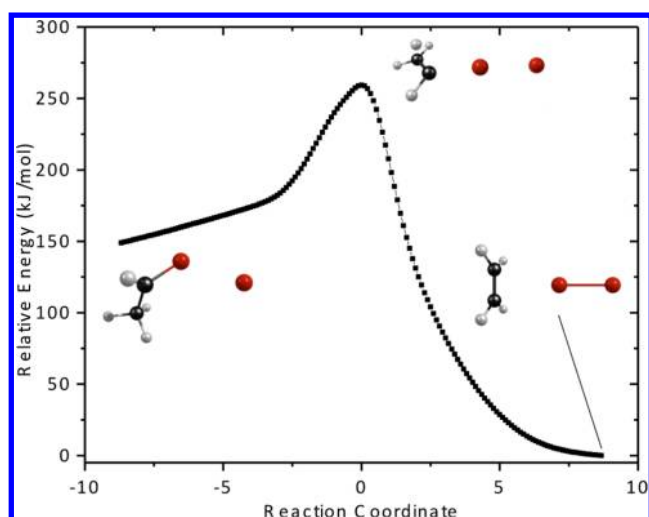


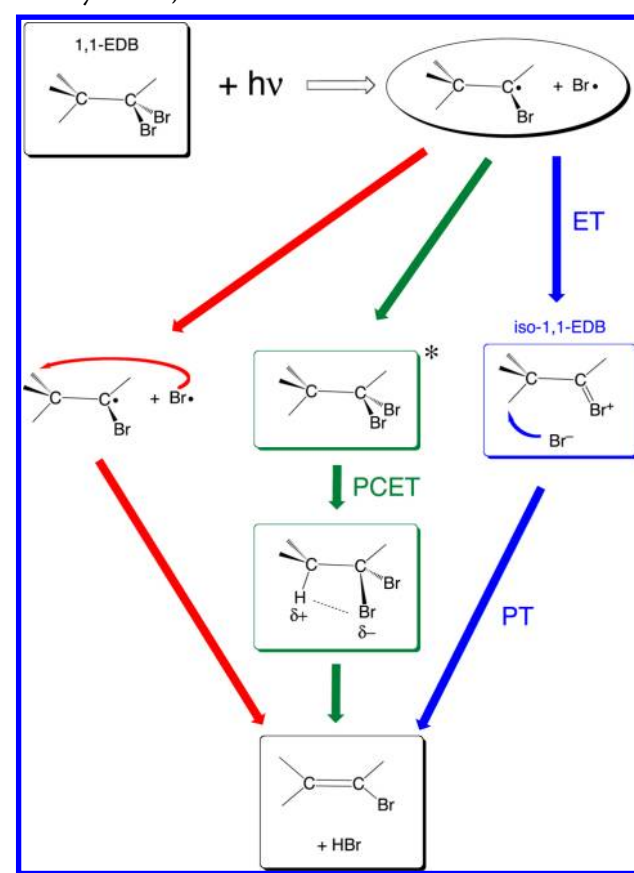
Figure 5. Intrinsic reaction coordinate calculation of the reaction paths linking iso-1,1-dibromoethane to the elimination of Br_2 , performed at the M062x/aug-cc-pVTZ level.

therefore carried out additional experiments at a longer wavelength of 240 nm, where the radical and iso-1,1-EDB are predicted to absorb only weakly (Table 2). Unfortunately, the parent 1,1-EDB also absorbs quite weakly at this wavelength (Figure 2), and longer photolysis times (i.e., several hours) were required. Nonetheless, the results were similar; details are provided in Figure S3 in the Supporting Information.

Additional information on the relative importance of secondary photolysis comes from experiments on the 1,1-DB-2,2,2-TFE analogue, where the isomer is the only observed photoproduct (Figure 3). The calculated (TDDFT) spectra of the 1-bromo-2,2,2-trifluoroethyl radical show a strong absorption at 247 nm, near our 240 nm photolysis wavelength. We emphasize that the efficiency of secondary photolysis will necessarily depend on the lifetime of the intermediate, which is expected to be very short (ps to sub-ps time scale) in the case of these radicals, based on ultrafast measurements of the condensed phase recombination rates in similar systems.^{8,12,17,18,20,24,27}

Summarizing this part of our picture of the photolysis of 1,1-EDB in condensed phases, we suggest that the observed Br_2 elimination occurs primarily from the isomer via a concerted process. What, then, is the origin of the HBr photoproduct? In our previous theoretical study,³⁹ we showed that two pathways are possible for hydrogen halide elimination on the ground state of 1,1-EDB, both of which lie energetically below the radical channel: (1) a single-step pathway through a 4-center TS, which involves significant charge separation and can be considered as a concerted (simultaneous as opposed to stepwise) proton-coupled electron transfer (PCET) event, and (2) a higher energy sequential pathway where the first and rate-limiting step is an electron transfer (isomerization) accessing iso-1,1-EDB followed by proton transfer (ET/PT). Scheme 1 summarizes the possible pathways for formation of HBr and vinyl bromide in the condensed phase photolysis of 1,1-EDB, while Figure 4 shows the calculated stationary points relevant to these paths. As illustrated in Scheme 1, geminate recombination of the initially formed radical pair can lead to HBr via (a) a simple radical abstraction, (b) concerted PCET via a 4-center TS on the ground state following reformation of the parent, and (c) an ET/PT pathway, which involves the

Scheme 1. Possible Mechanisms for HBr Elimination in Photolysis of 1,1-EDB



isomer as an intermediate.³⁹ Our previous study has established that the latter two pathways involve significant charge separation and are best characterized as coupled electron/proton transfer.³⁹

There is a limited amount of information that steady-state experiments can provide as to the relative importance of these pathways in the photochemical reaction. However, we can argue against a simple radical abstraction mechanism on the following theoretical grounds. Our calculations show that the approach of a Br atom to the β -carbon of the 1-bromoethyl radical is associated with significant charge transfer to the approaching Br atom. A relaxed redundant scan of the Br–H distance taken with the Br–H–C angle fixed as linearity is shown in Figure 6, where both the relative energy and (Merz–Kollman,^{52,53} MK) charge on the approaching Br atom are plotted. While there is no barrier for the abstraction, significant charge transfer occurs and geometries similar to the optimized structure of the 4-center PCET TS are accessed.³⁹ For example, the Br–C–C angle decreases from 103° at $R_{\text{Br-H}} = 4 \text{ \AA}$ to 76° at $R_{\text{Br-H}} = 1.6 \text{ \AA}$, where the C–H bond is substantially broken (Figure 6). In the 4-center TS structure optimized at the M062x/aug-cc-pVTZ level, this angle is 84° .³⁹ These observations are consistent with PCET, occurring through a concerted transition state with significant ion-pair character, being the kinetically favored pathway for HBr elimination on the 1,1-EDB ground state PES.³⁹ Radical recombination leading directly back to the parent will access this pathway preferentially (Scheme 1), as will recombination trajectories that initially lead to isomer formation with subsequent back-isomerization. From the isomer well, back-isomerization

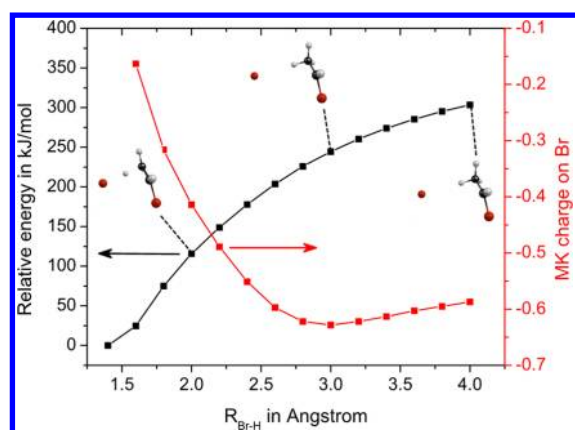


Figure 6. Relaxed energy scan at the M062/aug-cc-pVTZ level illustrating a hypothetical reaction pathway for H atom abstraction by Br from the CH_3CHBr radical. In this case, the angle of approach is fixed by restricting the Br–H–C angle to linearity. This scan shows that there is no barrier to reaction but also that the reaction involves significant charge transfer, as indicated by the partial charge on the approaching Br atom.

competes with a sequential ET/PT mechanism for dehydrohalogenation (Figure 4). The relative importance of these pathways can be judged if the quantum yield for isomer formation from the dissociated products is known. In related polyhalomethanes, these yields can be substantial; e.g., ultrafast experiments show that the quantum yield of iso- CH_2BrI formation in the photolysis of CH_2BrI in solution is 0.26 (100 ps after excitation).⁵⁴

Thus far, we have assumed that the chemistry occurs solely on the singlet PESs. However, the role of the triplet surfaces should also be considered. To gauge the potential influence of the triplet surfaces, we performed fully relaxed scans along the C–Br–Br bond angle, in both the ground singlet and first excited triplet states. Note that this scan is an excellent mimic of the isomerization reaction coordinate.²³ As shown in Figure 7, which displays scans calculated at the MP2/aug-cc-pVTZ

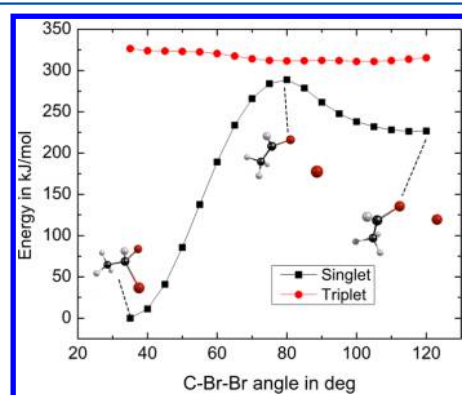


Figure 7. Scans of the lowest singlet and triplet states of 1,1-EDB along the C–Br–Br angle, which approximates the isomerization reaction coordinate.

level, we find that there is essentially no barrier to the isomerization on the lowest triplet surface, so that the triplet and singlet PESs approach near the isomerization barrier on the singlet surface. The triplet, of course, is a true biradical, while the singlet is mainly described as an ion pair, with maximal charge on the isomerizing Br atom in the barrier region.²³

Finally, it is instructive to compare the condensed phase photochemistry of 1,1-EDB with that of the structural isomer 1,2-EDB.³⁶ In the latter case, the primary photoproduct observed in the matrix was $\text{Br}_2 + \text{C}_2\text{H}_4$, again observed as a complex, with only a trace amount of HBr detected. In this case, as in the gas-phase studies, the photon energy is sufficient to break both C–Br bonds (sequentially), and simple recombination leads to the Br_2 (+ ethylene) product. However, the observation of HBr suggests a small contribution from a PCET pathway analogous to that characterized here. In this case, HBr loss would compete with formation of an ion pair involving a cyclic bromonium ion, which could react to reform parent or eliminate Br_2 following back ET. Such a pathway has been previously invoked to explain the prompt I_2 yield observed in ultrafast studies of 1,2-diiodoethane in solution.²⁷

CONCLUSIONS

We have explored the photodissociation of matrix isolated 1,1-dibromoethane (1,1-EDB) and observed photoproducts consistent with elimination to molecular products HBr (+ vinyl bromide) and Br_2 (+ ethylene or acetylene). In contrast, the iso-1,1-EDB species, while demonstrated computationally to be a minimum on the 1,1-EDB PES, could not be trapped. Indirect evidence for the formation of the isomer was found in experiments on the 2,2,2-trifluorinated analogue, where the isomer is the only observed photoproduct.

We have investigated theoretically the different molecular elimination channels. For Br_2 elimination, a pathway from the iso-1,1-EDB species was found, which involves a concerted Br_2 loss with 1,2-hydrogen shift. This pathway lies much lower in energy than a concerted three-center elimination pathway from 1,1-EDB. In this case, we argue against a simple radical abstraction since approach of the liberated Br radical to the bound Br must transiently access the isomer well on the PES. For the HBr elimination pathway, there are distinct pathways occurring on the ground PES, which involved concerted and sequential proton coupled electron transfer, with the sequential pathway involving iso-1,1-EDB as a key intermediate. While a simple radical pathway for the H-abstraction can be envisioned, our calculations show that this pathway involves significant charge transfer and accesses geometries similar to the TS for concerted PCET.

The results reported here provide a valuable foundation for subsequent studies of the photochemistry of this molecule. It is surprising that ultrafast studies of this molecule have not, to our knowledge, been reported. The participation of the iso-1,1-EDB species can be examined by probing on its intense near-UV absorption band, predicted to lie near 350 nm (Table 2). The HBr photoproduct can be probed in the IR region. Molecular dynamics simulations may also be helpful in probing the mechanisms of molecular elimination. From our point of view, such reactions will usually involve coupled proton and electron transfer.

ASSOCIATED CONTENT

Supporting Information

Three figures and four tables of additional experimental and computational data. This material is available free of charge via the Internet at <http://pubs.acs.org>.

AUTHOR INFORMATION

Corresponding Author

*(S.A.R.) E-mail: scott.reid@mu.edu.

Notes

The authors declare no competing financial interest.

■ ACKNOWLEDGMENTS

We acknowledge many valuable discussions with Prof. Rajendra Rathore. Support of the National Science Foundation (grant CHE-1057951), the Donors of the Petroleum Research Fund of the American Chemical Society (grant 48740-ND6), and the NSF funded Pere cluster at Marquette is acknowledged.

■ REFERENCES

- (1) Ballschmiter, K. Pattern and Sources of Naturally Produced Organohalogens in the Marine Environment: Biogenic Formation of Organohalogens. *Chemosphere* **2003**, *52*, 313–324.
- (2) Schmidberger, J. W.; James, A. B.; Edwards, R.; Naismith, J. H.; O'Hagan, D. Halomethane Biosynthesis: Structure of a Sam-Dependent Halide Methyltransferase from *Arabidopsis thaliana*. *Angew. Chem., Int. Ed.* **2010**, *49*, 3646–3648.
- (3) Gribble, G. W. Natural Organohalogens: A New Frontier for Medicinal Agents? *J. Chem. Educ.* **2004**, *81*, 1441–1449.
- (4) Gribble, G. W. The Diversity of Naturally Produced Organohalogens. *Chemosphere* **2003**, *52*, 289–297.
- (5) Maier, G.; Reisenauer, H. P. Photoisomerization of Dihalomethanes. *Angew. Chem., Int. Ed.* **1986**, *25*, 819–822.
- (6) Maier, G.; Reisenauer, H. P.; Hu, J.; Schaad, L. J.; Hess, B. A. Photochemical Isomerization of Dihalomethanes in Argon Matrices. *J. Am. Chem. Soc.* **1990**, *112*, 5117–5122.
- (7) Li, Y. L.; Zhao, C.; Kwok, W. M.; Guan, X.; Zuo, P.; Phillips, D. L. Observation of a HI Leaving Group Following Ultraviolet Photolysis of CH_2I_2 in Water and an Ab Initio Investigation of the O–H Insertion/HI Elimination Reactions of the $\text{CH}_2\text{I}\cdot$ Isopolyhalomethane Species with H_2O and $2\text{H}_2\text{O}$. *J. Chem. Phys.* **2003**, *119*, 4671–4681.
- (8) Wall, M.; Tarnovsky, A. N.; Pascher, T.; Sundstrom, V.; Akesson, E. Photodissociation Dynamics of Iodoform in Solution. *J. Phys. Chem. A* **2003**, *107*, 211–217.
- (9) Kwok, W. M.; Zhao, C. Y.; Li, Y. L.; Guan, X. G.; Phillips, D. L. Direct Observation of an Isopolyhalomethane O–H Insertion Reaction with Water: Picosecond Time-Resolved Resonance Raman (Ps-Tr3) Study of the Isobromomethane Reaction with Water to Produce a CHBr_2OH Product. *J. Chem. Phys.* **2004**, *120*, 3323–3332.
- (10) Kwok, W. M.; Zhao, C.; Li, Y.-L.; Guan, X.; Wang, D.; Phillips, D. L. Water-Catalyzed Dehalogenation Reactions of Isobromomethane and Its Reaction Products. *J. Am. Chem. Soc.* **2004**, *126*, 3119–3131.
- (11) Phillips, D. L.; Fang, W. H.; Zheng, X.; Li, Y. L.; Wang, D.; Kwok, W. M. Isopolyhalomethanes: Their Formation, Structures, Properties and Cyclopropanation Reactions with Olefins. *Curr. Org. Chem.* **2004**, *8*, 739–755.
- (12) Tarnovsky, A. N.; Sundstrom, V.; Akesson, E.; Pascher, T. Photochemistry of Diiodomethane in Solution Studied by Femtosecond and Nanosecond Laser Photolysis. Formation and Dark Reactions of the $\text{CH}_2\text{I}\cdot$ Isomer Photoproduct and Its Role in Cyclopropanation of Olefins. *J. Phys. Chem. A* **2004**, *108*, 237–249.
- (13) Guan, X. G.; Lin, X. F.; Kwok, W. M.; Du, Y.; Li, Y. L.; Zhao, C. Y.; Wang, D. Q.; Phillips, D. L. Ultraviolet Photolysis of CH_2I_2 in Methanol: O–H Insertion and HI Elimination Reactions to Form a Dimethoxymethane Product. *J. Phys. Chem. A* **2005**, *109*, 1247–1256.
- (14) Li, Y. L.; Zhao, C.; Guan, X.; Phillips, D. L. Ab Initio Investigation of the O–H Insertion Reactions of $\text{CH}_2\text{X}\cdot$ ($\text{X} = \text{Cl}, \text{Br}, \text{I}$) Isopolyhalomethanes with Water. *Res. Chem. Intermed.* **2005**, *31*, 557–565.
- (15) Lin, X. F.; Guan, X. G.; Kwok, W. M.; Zhao, C. Y.; Du, Y.; Li, Y. L.; Phillips, D. L. Water-Catalyzed O–H Insertion/HI Elimination Reactions of Isodihalomethanes ($\text{CH}_2\text{X}\cdot$, Where $\text{X} = \text{Cl}, \text{Br}, \text{I}$) with Water and the Dehalogenation of Dihalomethanes in Water-Solvated Environments. *J. Phys. Chem. A* **2005**, *109*, 981–998.
- (16) Lin, X. F.; Zhao, C. Y.; Phillips, D. L. An Ab Initio Study of the Reactions of $\text{CH}_2\text{X}\cdot$ ($\text{X} = \text{Cl}, \text{Br}, \text{I}$) Isopolyhalomethanes with CH_3OH . *Mol. Simul.* **2005**, *31*, 483–488.
- (17) Tarnovsky, A. N.; Pascher, I.; Pascher, T. Reactivity of iso-Diiodomethane and iso-Iodoform, Isomers of CH_2I_2 and CHI_3 , toward the Double Bond of a Variety of Cycloalkenes. *J. Phys. Chem. A* **2007**, *111*, 11814–11817.
- (18) El-Khoury, P. Z.; Kwok, W. M.; Guan, X. G.; Ma, C. S.; Phillips, D. L.; Tarnovsky, A. N. Photochemistry of Iodoform in Methanol: Formation and Fate of the iso- $\text{CHI}_2\cdot$ Photoproduct. *ChemPhysChem* **2009**, *10*, 1895–1900.
- (19) Carrier, S. L.; Preston, T. J.; Dutta, M.; Crowther, A. C.; Crim, F. F. Ultrafast Observation of Isomerization and Complexation in the Photolysis of Bromoform in Solution. *J. Phys. Chem. A* **2010**, *114*, 1548–1555.
- (20) El-Khoury, P. Z.; George, L.; Kalume, A.; Ault, B. S.; Tarnovsky, A. N.; Reid, S. A. Frequency and Ultrafast Time Resolved Study of Iso- CF_2I_2 . *J. Chem. Phys.* **2010**, *132*, 124501.
- (21) George, L.; Kalume, A.; El-Khoury, P. Z.; Tarnovsky, A.; Reid, S. A. Matrix Isolation and Computational Study of Isodifluorodibromomethane ($\text{F}_2\text{CBr}\cdot$): A Route to Br_2 Formation in CF_2Br_2 Photolysis. *J. Chem. Phys.* **2010**, *132*, 084503.
- (22) Kalume, A.; George, L.; Reid, S. A. Isomerization as a Key Pathway to Molecular Products in the Gas-Phase Decomposition of Halons. *J. Phys. Chem. Lett.* **2010**, *1*, 3090–3095.
- (23) George, L.; Kalume, A.; Esselman, B. J.; Wagner, J.; McMahon, R. J.; Reid, S. A. Spectroscopic and Computational Studies of Matrix-Isolated iso- CHBr_3 : Structure, Properties, and Photochemistry of iso-Bromoform. *J. Chem. Phys.* **2011**, *135*, 124503.
- (24) Preston, T. J.; Dutta, M.; Esselman, B. J.; Kalume, A.; George, L.; McMahon, R. J.; Reid, S. A.; Crim, F. F. Formation and Relaxation Dynamics of iso- $\text{CH}_2\text{Cl}\cdot$ in Cryogenic Matrices. *J. Chem. Phys.* **2011**, *135*, 114503.
- (25) George, L.; Kalume, A.; Esselman, B.; McMahon, R. J.; Reid, S. A. Spectroscopic and Computational Properties of Matrix Isolated CXBr_3 ($\text{X} = \text{F}, \text{Cl}, \text{Br}$): Structure, Properties, and Photochemistry of iso-Tribromomethanes. *J. Mol. Struct.* **2012**, *1025*, 61–68.
- (26) Pal, S. K.; Mereshchenko, A. S.; Butaeva, E. V.; El-Khoury, P. Z.; Tarnovsky, A. N. Global Sampling of the Photochemical Reaction Paths of Bromoform by Ultrafast Deep-UV through near-IR Transient Absorption and ab Initio Multiconfigurational Calculations. *J. Chem. Phys.* **2013**, *138*, 124501.
- (27) Rasmusson, M.; Tarnovsky, A. N.; Pascher, T.; Sundstrom, V.; Akesson, E. Photodissociation of $\text{CH}_2\text{ICH}_2\text{I}$, $\text{CF}_2\text{ICF}_2\text{I}$, and $\text{CF}_2\text{BrCF}_2\text{I}$ in Solution. *J. Phys. Chem. A* **2002**, *106*, 7090–7098.
- (28) Kong, Q. Y.; Kim, J.; Lorenc, M.; Kim, T. K.; Ihee, H.; Wulff, M. Photodissociation Reaction of 1,2-Diiodoethane in Solution: A Theoretical and X-Ray Diffraction Study. *J. Phys. Chem. A* **2005**, *109*, 10451–10458.
- (29) Ihee, H.; Lorenc, M.; Kim, T. K.; Kong, Q. Y.; Cammarata, M.; Lee, J. H.; Bratos, S.; Wulff, M. Ultrafast X-Ray Diffraction of Transient Molecular Structures in Solution. *Science* **2005**, *309*, 1223–1227.
- (30) Kim, J.; Lee, J. H.; Kim, J.; Jun, S.; King, K. H.; Kim, T. W.; Wulff, M.; Ihee, H. Structural Dynamics of 1,2-Diiodoethane in Cyclohexane Probed by Picosecond X-ray Liquidography. *J. Phys. Chem. A* **2012**, *116*, 2713–2722.
- (31) Ji, L.; Tang, Y.; Zhu, R. S.; Wei, Z. R.; Zhang, B. Photodissociation Dynamics of Allyl Bromide at 234, 265, and 267 nm. *J. Chem. Phys.* **2006**, *125*, 164307.
- (32) Lee, H. L.; Lee, P. C.; Tsai, P. Y.; Lin, K. C.; Kuo, H. H.; Chen, P. H.; Chang, A. H. H. Photodissociation of Dibromoethanes at 248 nm: An Ignored Channel of Br-2 Elimination. *J. Chem. Phys.* **2009**, *130*, 184308.
- (33) Lee, Y. R.; Chen, C. C.; Lin, S. M. Photodissociation of CH_2Br_2 , 1,1- and 1,2- $\text{C}_2\text{H}_4\text{Br}_2$ at 248 nm: A Simple C–Br Bond Fission Versus a Concerted Three-Body Formation. *J. Chem. Phys.* **2003**, *118*, 10494–10501.

- (34) Tang, Y.; Ji, L.; Tang, B.-F.; Zhu, R.-S.; Zhang, S.; Zhang, B. Photodissociation of Alkyl Bromides at UV Scope. *Wuli Huaxue Xuebao* **2004**, *20*, 344–349.
- (35) Tang, Y.; Ji, L.; Tang, B. F.; Zhu, R. S.; Zhang, S.; Zhang, B. Studies on Photodissociation of Alkyl Bromides at 234 and 267 nm. *Chem. Phys. Lett.* **2004**, *392*, 493–497.
- (36) Kalume, A.; George, L.; El-Khoury, P. Z.; Tarnovsky, A. N.; Reid, S. A. Spectroscopic and Computational Studies of the Laser Photolysis of Matrix Isolated 1,2-Dibromoethanes: Formation and Fate of the Bromoethyl Radicals. *J. Phys. Chem. A* **2010**, *114*, 9919–9926.
- (37) George, L.; Wittmann, L.; Kalume, A.; Reid, S. A. Photoinduced Electron Transfer in a Prototypical Mulliken Donor–Acceptor Complex: $C_2H_4 \cdots Br_2$. *J. Phys. Chem. Lett.* **2010**, *1*, 2618–2620.
- (38) Nguyen, T.; Ollis, D. F. Complete Heterogeneously Photocatalyzed Transformation of 1,1-Dibromoethane and 1,2-Dibromoethane to CO_2 and HBr. *J. Phys. Chem.* **1984**, *88*, 3386–3388.
- (39) Kalume, A.; George, L.; Cunningham, N.; Reid, S. A. Concerted and Sequential Pathways of Proton-Coupled Electron Transfer in Hydrogen Halide Elimination. *Chem. Phys. Lett.* **2013**, *556*, 35–38.
- (40) Kjaergaard, H. G.; Robinson, T. W.; Brooking, K. A. Calculated CH-Stretching Overtone Spectra of Naphthalene, Anthracene and Their Cations. *J. Phys. Chem. A* **2000**, *104*, 11297–11303.
- (41) Frisch, M. J.; et al. *Gaussian 09*; Gaussian Inc.: Wallingford, CT, 2009.
- (42) Boys, S. F.; Bernardi, F. Calculation of Small Molecular Interactions by Differences of Separate Total Energies: Some Procedures with Reduced Errors. *J. Mol. Phys.* **1970**, *19*, 553–566.
- (43) Mokrushin, V.; Bedanov, V.; Tsang, W.; Zachariah, M.; Knyasev, V. *ChemRate*, 1.5.8 ed.; National Institute of Standards and Technology: Gaithersburg, MD, 2009.
- (44) Khundkar, L. R.; Marcus, R. A.; Zewail, A. H. Unimolecular Reactions at Low Energies and RRKM Behavior: Isomerization and Dissociation. *J. Phys. Chem.* **1983**, *87*, 2473–2476.
- (45) Maric, D.; Burrows, J. P.; Moortgat, G. K. A Study of the UV-Visible Absorption-Spectra of Br_2 and $BrCl$. *J. Photochem. Photobiol. A* **1994**, *83*, 179–192.
- (46) Tarnovsky, A. N.; Alvarez, J. L.; Yartsev, A. P.; Sundstrom, V.; Akesson, E. Photodissociation Dynamics of Diiodomethane in Solution. *Chem. Phys. Lett.* **1999**, *312*, 121–130.
- (47) Kwok, W. M.; Ma, C. S.; Parker, A. W.; Phillips, D.; Towrie, M.; Matousek, P.; Phillips, D. L. Picosecond Time-Resolved Resonance Raman Observation of the iso- CH_2I-I Photoproduct from the "Photoisomerization" Reaction of Diiodomethane in the Solution Phase. *J. Chem. Phys.* **2000**, *113*, 7471–7478.
- (48) Elles, C. G.; Crim, F. F. Connecting Chemical Dynamics in Gases and Liquids. *Annu. Rev. Phys. Chem.* **2006**, *57*, 273–302.
- (49) Miller, D. M.; Schreiner, P. R.; Schaefer, H. F. Singlet Methylcarbene: an Elusive Intermediate of the Thermal-Decomposition of Diazoethane and Methyl diazirene. *J. Am. Chem. Soc.* **1995**, *117*, 4137–4143.
- (50) Ma, B. Y.; Schaefer, H. F. Singlet Methylcarbene: Equilibrium Geometry or Transition-State. *J. Am. Chem. Soc.* **1994**, *116*, 3539–3542.
- (51) Chang, A. H. H.; Mebel, A. M.; Yang, X. M.; Lin, S. H.; Lee, Y. T. Ab Initio Calculations of Potential Energy Surface and Rate Constants for Ethylene Photodissociation at 193 and 157 nm. *Chem. Phys. Lett.* **1998**, *287*, 301–306.
- (52) Kollman, P. A.; Merz, K. M. Computer Modeling of the Interactions of Complex-Molecules. *Acc. Chem. Res.* **1990**, *23*, 246–252.
- (53) Besler, B. H.; Merz, K. M.; Kollman, P. A. Atomic Charges Derived from Semiempirical Methods. *J. Comput. Chem.* **1990**, *11*, 431–439.
- (54) Tarnovsky, A. N.; Wall, M.; Gustafsson, M.; Lascoux, N.; Sundstrom, V.; Akesson, E. Ultrafast Study of the Photodissociation of Bromiodomethane in Acetonitrile Upon 266 nm Excitation. *J. Phys. Chem. A* **2002**, *106*, 5999–6005.